arXiv:0803.0258v1 [hep-ph] 3 Mar 2008

CERN-PH-TH/2008-030
DESY 08-028
SHEP-08-08

Evidence for the Discrete Asymptotically-Free BFKL Pomeron from HERA Data

J. Ellis [1], H. Kowalski [2] and D.A. Ross [1,3]

[1] *Theory Division, Physics Department, CERN, CH-1211 Geneva 23, Switzerland*

[2] *Deutsches Elektronen-Synchrotron DESY, D-22607 Hamburg, Germany*

[3] *School of Physics and Astronomy, University of Southampton Highfield, Southampton SO17 1BJ, UK*

Abstract

We show that the next-to-leading-order renormalization-group-improved asymptotically-free BFKL Pomeron provides a good fit to HERA data on virtual photoproduction at small x and large Q^2. The leading discrete Pomeron pole reproduces qualitatively the Q^2 dependence of the HERA data for $x \sim 10^{-3}$, and a fit using the three leading discrete singularities reproduces quantitatively the Q^2 and x dependence of the HERA data for $x < 10^{-2}$. This fit fixes the phase for all the BFKL wavefunctions at a chosen infrared scale.

CERN-PH-TH/2008-030
February 2008

The nature of the QCD Pomeron continues to perplex and intrigue both experimentalists and theorists [1]. Study of the Pomeron has been one of the most interesting aspects of the HERA experimental programme, with the discovery of a 'hard' Pomeron in virtual photoproduction [2] whose relation to the 'soft' Pomeron that is familiar from traditional hadronic reactions [3] is still the subject of theoretical speculation. In the near future, the LHC will provide possibilities to test theoretical approaches that have been honed with HERA data and may provide novel opportunities to study new Pomeron physics.

Most of the HERA data on deep-inelastic structure functions are described well by the asymptotically-free renormalization-group evolution expressed in the Dokshitzer-Gribov-Lipatov-Altarelli-Parisi (DGLAP) [4] equations. On the other hand, it has been suggested that a more appropriate framework for describing data at very low x is the diffusion in transverse momentum incarnated in the Balitsky-Fadin-Kuraev-Lipatov (BFKL) equation [5]. There has been considerable discussion of HERA data at low x in the context of unified BFKL and DGLAP equations [6]. However, it has not yet been established whether the *pure* BFKL Pomeron provides an accurate description of data in the kinematic range accessible to HERA.

The BFKL equation with fixed strong coupling yields a leading Pomeron singularity that is a Regge cut, not a pole. Fixing the QCD coupling may be plausible in a suitable infra-red limit, but the coupling runs significantly in the ranges of virtuality and transverse parton momenta explored in inclusive measurements of structure functions at HERA. Over 20 years ago, it was shown [7] that within the BFKL formalism, the leading Pomeron singularity is a discrete Regge pole if the strong QCD coupling is treated correctly as asymptotically free and the infrared behaviour is encoded in a fixed phase. This leading singularity is followed by an infinite series of lower-lying poles.

The next-to-leading-order (NLO) QCD correction to the leading-order (LO) asymptotically-free BFKL equation is known [8], and it has been shown how to re-sum higher-order corrections so as to tame the NLO corrections [9]. The asymptotically-free BFKL equation described in [7] describes *both* the x- dependence of the un-integrated gluon distribution and the dependence on the transverse momentum, k, of the gluon, and hence also the Q^2 dependence of the structure function at low x. The only unknown quantity is the proton impact factor, $\Phi_p(k)$, which describes the couplings of the proton to the Pomeron trajectories. One benefit of the discrete Pomeron approach is that a simple expression for the un-integrated gluon density can be obtained, in terms of a small number of parameters, by expanding the proton impact factor in terms of the discrete set of solutions of the asymptotically-free BFKL equation. We recall that the BFKL Pomeron may be expressed as an integral that includes DGLAP as a saddle-point approximation valid in the double limit $\ln(1/x) \gg 1$ and $\alpha_s(Q^2)\ln(1/x) \ll 1$ [10]. However, this DGLAP approximation to the BFKL integral is no longer valid when the second condition is not satisfied, as in the case of low-x HERA data, where the discrete series of BFKL Pomeron Regge poles is a better systematic approximation scheme.

We are unaware of any overall fit to HERA data made using the re-summed NLO asymptotically-free BFKL Pomeron. We perform such a fit in this paper, and show that it describes the inclusive virtual photoproduction HERA data both qualitatively and quantita-

tively. We show first that the leading BFKL Pomeron pole provides a successful qualitative description of HERA data on inclusive virtual photoproduction at small $x \sim 10^{-3}$, over a large range of Q^2. This fit improves if lower-lying BFKL Pomeron poles are included, and we show that the asymptotically-free BFKL approach provides an excellent quantitative fit to all the inclusive HERA data at $x \leq 10^{-2}$, if the three leading BFKL Pomeron Regge poles are included. As well as the residues of the three BFKL Pomeron poles at zero momentum transfer, t, the BFKL fit has an additional free parameter corresponding to the value of the phase of the BFKL wave function that is assumed to be fixed by infra-red dynamics at a momentum $k_0 \sim 0.3$ GeV [1].

We consider first the BFKL analysis of a zero-momentum-transfer process, at fixed strong coupling, α_s. In this case, the eigenfunctions of the BFKL kernel are representations of the two-dimensional conformal group in the space of the transverse coordinates of the gluons, ρ. We include the BFKL characteristic function up to NLO [8], and use the re-summation of Scheme 3 proposed by Salam [9], which moderates the correction to the leading intercept as well as preserving the sign of the curvature of the characteristic function near the intercept, up to large values of α_s.

Considering only the leading conformal spin, the eigenfunctions may be written in momentum space as

$$f_\omega(k^2) \;=\; \frac{\overline{f_\omega}(k)}{\sqrt{k^2}}, \tag{1}$$

with

$$\overline{f_\omega}(k) \;= \left(k^2\right)^{i\nu}, \tag{2}$$

where the eigenvalue ω is the solution to the equation

$$\omega \;\equiv\; \chi(\alpha_s,\nu) \;=\; \bar{\alpha}_s\left(1 - A\bar{\alpha}_s\right)\overline{\chi_0}\left(\frac{1}{2} + \bar{\alpha}_s B + \frac{\omega}{2} + i\nu\right) + \bar{\alpha}_s^2\overline{\chi_1}(\nu). \tag{3}$$

Here

$$\bar{\alpha}_s \;\equiv\; \frac{C_A}{\pi}\alpha_s,$$

$$\overline{\chi_0}(z) = 2\left(\psi(1) - \Re e\left[\psi(z)\right]\right)$$

$$A \;\equiv\; \frac{n_f}{36C_A^3}\left(10C_A^2 + 13\right) - \frac{\pi^2}{6},$$

and

$$B \;=\; \frac{11}{8} - \frac{n_f}{12C_A^3}\left(C_A^2 - 2\right),$$

where $C_A = 3$ and n_f is the number of active flavours at momentum k. $\overline{\chi_1}(\nu)$ is the NLO characteristic function given in [8], omitting the conformal symmetry-violating part associated with the running of the coupling (which is subtracted so that the $\mathcal{O}(\bar{\alpha}_s^2)$ terms on the RHS of (3) are not double-counted: see [9]). The implicit equation (3) for ω is readily solved using an appropriate combination of Newton's method and iteration.

[1] The precise value of k_0 is not an essential parameter.

Turning now to the case of running coupling, it was shown in [7] that the frequency ν of the oscillations acquires a dependence on k, such that for a fixed eigenvalue ω, $\nu_\omega(k) = \chi^{-1}(\omega, \alpha_s(k))$ is the solution to

$$\omega \ = \chi\left(\alpha_s(k), \nu_\omega(k)\right). \tag{4}$$

This leads immediately to a critical value of the transverse momentum, $k_{\rm crit}$, such that

$$\omega \ = \ \chi(\alpha_s(k_{\rm crit}), 0). \tag{5}$$

Provided $\chi''(\alpha_s(k_{\rm crit}), 0)$ is negative [2], the value of $\nu_\omega(k)$ becomes imaginary for $k > k_{\rm crit}$ and the eigenfunction decreases exponentially as $k \to \infty$. It is in order to ensure that $\chi''(\alpha_s(k_{\rm crit}), 0)$ remains negative that we have opted for Scheme 3 of the re-summation procedure described in [9].

For $k \sim k_{\rm crit}$, the BFKL equation may be approximated as

$$\left[\frac{d^2}{d[\ln(k^2/k_{\rm crit}^2)]^2} + \frac{\beta_0}{2\pi}\frac{\dot\chi(\alpha_s(k_{\rm crit}), 0)}{\chi''(\alpha_s(k_{\rm crit}), 0)}\ln\left(\frac{k^2}{k_{\rm crit}^2}\right)\right]\overline{f_\omega}(k) \ = \ 0, \tag{6}$$

with

$$\beta_0 \ = \frac{11C_A}{3} - \frac{2}{3}n_f.$$

We recognize this as Airy's equation with argument proportional to $\ln(k^2/k_{\rm crit}^2)$. Away from $k_{\rm crit}$, provided the running of the coupling is not too fast, so that

$$\frac{d\nu_\omega(k)}{d\ln(k^2)} \ \ll \ \nu_\omega(k),$$

the BFKL equation may be approximated semi-classically by

$$\left[i\frac{d}{d\ln(k^2)} + \nu_\omega(k)\right]\overline{f_\omega}(k) \ = \ 0, \tag{7}$$

which has the solutions

$$\overline{f_\omega}(k) \ = \ e^{\pm i\varphi_\omega(k)}, \tag{8}$$

where

$$\varphi_\omega(k) \ = \ 2\int_k^{k_{\rm crit}}\frac{dk'}{k'}\left|\nu_\omega(k)\right|. \tag{9}$$

In all regions, the solutions *decrease* as $k \to \infty$, and are well approximated by

$$\overline{f_\omega}(k) = \sqrt{3}\sqrt[3]{\varphi_\omega(k)}K_{\frac{1}{3}}(\varphi_\omega(k)) \qquad (k > k_{\rm crit}), \tag{10}$$

whereas

$$\overline{f_\omega}(k) = \sqrt[3]{\varphi_\omega(k)}\left[J_{\frac{1}{3}}(\varphi_\omega(k)) + J_{-\frac{1}{3}}(\varphi_\omega(k))\right] \qquad (k < k_{\rm crit}), \tag{11}$$

[2] We use the notations $\chi''(\alpha_s, \nu) \equiv d^2\chi(\alpha_s, \nu)/d\nu^2$ and $\dot\chi(\alpha_s, \nu) \equiv d\chi(\alpha_s, \nu)/d\alpha_s$.

where we have expressed the appropriate Airy function in terms of the modified Bessel function of the second kind, $K_{\frac{1}{3}}$, and Bessel functions of the first kind, $J_{\pm\frac{1}{3}}$. Away from $k \sim k_{crit}$ where φ_ω becomes large, these Bessel function solutions approximate the solution to the semi-classical equation (7).

It is important to note that the matching of the solutions at $k = k_{\rm crit}$ determines the phase of the oscillations in the region where $k < k_{\rm crit}$, for a given value of ω. Following [7], we encode the unknown infrared behaviour of QCD by assuming that it leads to a fixed phase, η, at some low value of the transverse momentum, k_0, which we take for definiteness to be 0.3 GeV [3]. More precisely, the infrared condition is given by

$$\varphi_\omega(k_0) \;\equiv\; 2\int_{k_0}^{k_{\rm crit}} \frac{dk'}{k'}\,|\nu_\omega(k)| \;=\; \left(n-\frac{1}{4}\right)\pi + \eta, \tag{12}$$

and means that, just above $k = k_0$, the wavefunction behaves like

$$\overline{f_\omega}(k) \;\sim\; \sin\left(\frac{\nu_\omega(k_0)}{k_0^2}\left(k^2-k_0^2\right)-\eta\right). \tag{13}$$

Once the phase condition (12) is imposed, only a discrete set of values of the eigenvalue ω are allowed simultaneously by the infrared phase condition *and* the phase condition imposed by the matching, giving rise to a description of the QCD Pomeron as a discrete set of isolated poles, as opposed to the cut found if the running of the strong coupling is neglected.

In order to express the low-x structure function of the proton, $F_2(x,Q^2)$, in terms of these eigenfunctions, the eigenfunctions themselves must be convoluted with the impact factor $\Phi_p(k)$, that describes how the proton couples to these trajectories at zero momentum transfer. In the case of the un-integrated gluon density $xg(x,k)$, we have

$$xg(x,k) \;=\; \sum_n \int \frac{dk'}{k'}\Phi_p(k')x^{-\omega_n}k^2 f^*_{\omega_n}(k')f_{\omega_n}(k), \tag{14}$$

and the un-integrated gluon density is related to the structure function by

$$F_2(x,Q^2) \;=\; \int_0^Q \frac{dk}{k}\Phi_{\rm DIS}(Q,k)xg(x,k), \tag{15}$$

where the impact factor, $\Phi_{\rm DIS}$, that describes the coupling of the virtual photon to the trajectories is given by (see [1])

$$\Phi_{\rm DIS}(Q,k) \;=\; Q^2\alpha_s(Q^2)\sum_{q=1}^{n_f} e_q^2 \int_0^1 d\rho d\tau \frac{1-2\rho(1-\rho)-2\tau(1-\tau)+12\rho(1-\rho)\tau(1-\tau)}{Q^2\rho(1-\rho)+k^2\tau(1-\tau)}. \tag{16}$$

The proton impact factor, $\Phi_p(k)$ is unknown *a priori* and has to be fit to data. Since the eigenfunctions $f_{\omega_n}(k)$ form an orthonormal set, we can expand the impact factor as a series in these eigenfunctions with a discrete set of coefficients, a_n:

$$\Phi_p(k) \;= \sum_n a_n k^2 f_{\omega_n}(k), \tag{17}$$

[3] A change in this value of the infrared momentum scale can be compensated by a change in the phase, η, so that the infrared behaviour of QCD is in fact encoded using a single parameter.

and exploit the orthogonality properties to write

$$xg(x,k) \;=\; \sum_n a_n x^{-\omega_n} k^2 f_{\omega_n}(k). \tag{18}$$

A model for $\Phi_p(k)$ could be used to estimate the coefficients a_n, which could be also constrained using other HERA data, e.g., on the diffractive production of vector mesons.

At sufficiently small x, we expect this sum to be dominated by the first few poles. The contribution from the remaining poles could be approximated by assuming that the effect of fixing the phase at k_0 on the allowed values of ω is negligible for $\omega < 0.1$, and that the discrete set of eigenfunctions may be replaced by a continuum. In this case, one simply adds to the expression (18) for the un-integrated gluon density the following integral that represents the contribution from such a continuum:

$$xg(x,k)^{(\text{continuum})} \;=\; k\int_0^\infty d\nu\, b_p(\nu)\sin\left(\nu\ln\left(\frac{k^2}{k_0^2}\right)-\eta\right)x^{-\chi(\alpha_s(k^2),\nu)}\theta\left(0.1-\chi(\alpha_s(k^2),\nu)\right), \tag{19}$$

where $b_p(\nu)$ is a function that encodes the coupling of the proton to all the remaining eigenfunctions, and is chosen to be real so that the wavefunctions in this continuum also respect the imposed infrared condition (13). In order to implement such a programme one would need additional parameters to characterize the arbitrary function $b_p(\nu)$. However, in the region of x and Q^2 considered, we find an excellent fit without making use of such a continuum and the associated extra parameters, and hence do not consider it further. Nevertheless, it should be emphasized that at Q^2 that is sufficiently large for the DGLAP analysis to become valid, the double-leading-logarithm DGLAP behaviour would be embedded mainly within this continuum contribution.

We have determined numerically the eigenfunctions of the leading four poles of the NLO asymptotically-free BFKL Pomeron. We limited ourselves to the first four poles because their ω values are in the same range as the observed rate of rise, λ, of the F_2 measurements. This is determined by fitting the measured F_2 to $x^{-\lambda}$ at fixed Q^2 and is closely related to the logarithmic derivative $d\log(F_2)/d\log(1/x)$. The values of λ determined phenomenologically by experiment vary between $\lambda \approx 0.1$ for $Q^2 \leq 0.6$ GeV^2 and $\lambda \approx 0.33$ for $Q^2 \geq 60$ GeV^2 [11]. The leading eigenvalue, ω_1, depends on the infrared phase, η, varying between $\omega_1 = 0.235$ at $\eta = 0$ and $\omega_1 = 0.315$ at $\eta = \pi/2$, The sub-leading eigenvalues are smaller, the fourth one, ω_4, being ≈ 0.10.

We determined simultaneously the best-fit value of the infrared phase η and the coefficients, a_n. The fit was performed in the low-x region, $x \leq 0.01$ and for $Q^2 > 4$ GeV^2, so as to avoid saturation effects. The saturation scale at HERA was found to be $Q^2 \sim 0.5$ GeV^2 [12], implying that saturation effects should fall below the measurement precision for $Q^2 > 4$ GeV^2 [13]. The best fit is obtained for $\eta = -0.21\pi$, with the values for the first four eigenvalues and their corresponding k_{crit}, given in Table 1 ; the corresponding eigenfunctions (normalized in the domain $k > k_0$) are shown in Fig. 1. We see that the eigenvalues indeed decrease as n increases, so that for sufficiently small x the leading trajectories should be sufficient to describe the data over any fixed range in k. We note also that the eigenvalues approach each other as n increases.

n	ω	$k_{\rm crit}$ (GeV)
1	0.26	5.9
2	0.17	330
3	0.13	2.8×10^4
4	0.10	2.6×10^6

Table 1: *The eigenvalues and values of k_{crit} for the 4 leading eigenfunctions of the asymptotically-free BFKL Pomeron, for $\eta = -0.21\pi$ at $k_0 = 0.3$ GeV.*

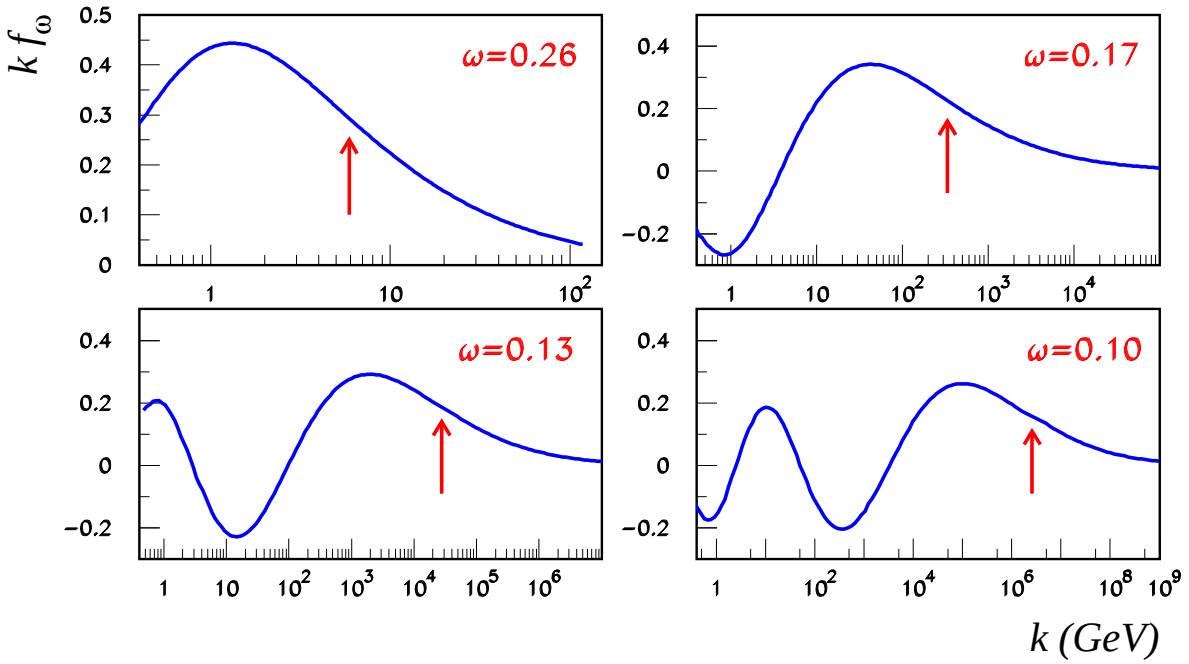


Figure 1: *The first four eigenfunctions of the NLO BFKL kernel with running coupling and infrared phase $\eta = -0.21\pi$ at $k_0 = 0.3$ GeV. The arrows indicate the values of k_{crit}.*

Number of poles	χ^2/N_{df}	a_1	a_2	a_3	a_4
1	3624/101	0.035	-	-	-
2	264/100	0.029	-0.028	-	-
3	91.4/99	0.041	0.055	0.085	-
4	91.3/98	0.042	0.067	0.11	0.016

Table 2: *The qualities of fits using up to 4 poles, and the corresponding pole residues, assuming $\eta = -0.21\pi$ at $k_0 = 0.3$ GeV.*

Having fixed the value of η, we investigate the number of eigenfunctions required for a good description of the HERA data for $x \leq 10^{-2}$. An overall 1-pole fit using only the leading eigenfunction has very poor quality: $\chi^2/N_{df} = 3624/101$, though it does reproduce qualitatively the data for $x \sim 10^{-3}$, where it is more likely to dominate over the non-leading Pomeron poles. The quality of the overall fit improves significantly when the two first eigenfunctions are used: $\chi^2/N_{df} = 264/100$, and the 3-pole fit is excellent: $\chi^2/N_{df} = 91.4/99$. On the other hand, adding a fourth eigenfunction does not improve the fit any further: $\chi^2/N_{df} = 91.3/98$. Since also the coefficient of the leading eigenfunction, a_1, is almost the same in the 3- and 4-pole fits, in the following we consider only the fits with 3 or less eigenfunctions.

Fig. 2 compares the results of the 1- and 3-pole fits with the measured values of F_2. We see that the 3-pole fit indeed describes the data very well, corresponding to its very good χ^2. Fig. 2 also displays the 1-pole fit; despite its very high χ^2, it reproduces qualitatively the main features of the data, particularly for moderate Q^2. We note that the coefficient, a_1, of the leading eigenfunction in the 1-pole fit is about 20% *smaller* than in the 3-pole fit. This indicates that the excellent agreement of the 3-pole fit with the data is due in part to cancellations between the different eigenfunctions. To illustrate the properties of the 3-pole fit, we show in Fig. 3 the contributions to F_2 from the 3 eigenfunctions separately as functions of the momenta k^2 at several characteristic x values. Fig. 3 shows that, in the region of medium Q^2 values: $4 < Q^2 < 20$ GeV^2, the contribution of the leading eigenfunction coincides with the fitted F_2 curve, i.e., the contributions of the second and third eigenfunctions cancel each other. However, at larger Q^2, especially above $Q^2 > 100$ GeV^2, the fit has large cancellations between all three components, and the leading eigenfunction cannot fit the data by itself.

Fig. 4 compares the Q^2 dependence of the effective value of the exponent λ determined from a phenomenological fit to the data, and as extracted from our fits [4]. In the case of the 1-pole fit (dashed line), λ is identical with the leading eigenvalue: $\omega = 0.26$, and in the 2-pole fit (dotted line) the values of λ become mostly smaller than the leading eigenvalue. However, in the 3-pole fit, whilst the λ values are smaller than the leading eigenvalue for $Q^2 < 20$ GeV^2 (solid line), they become larger at higher Q^2, and are closer to the values extracted form a phenomenological fit to the data. The surprising fact that the sum of the contribution with small eigenvalues can give a larger rate of rise than the leading eigenvalue is due to the fact that λ is closely connected to the logarithmic derivative, $\lambda \approx d\log(F_2)/d\log(1/x)$. Owing to these cancellations, the logarithmic derivative can become larger than the largest eigenvalue. The fact that the 3-pole BFKL fit gives somewhat smaller values of λ than the phenomenological fit for $Q^2 \sim 20$ to 70 GeV^2 is closely related to the fact that the lowest-x point at each of these values of Q^2 lies slightly above the 3-pole fit, as seen in the corresponding panels of Fig. 2. However, the minor discrepancies for these few points does not spoil the quality of the overall fit, which is a better measure of its validity than the λ plot shown in Fig. 4.

In summary: we obtain a very good description of the HERA low-x data in a large range

[4] In Fig. 4 we have also included recent data from Zeus [14] which are fully consistent with previous data, and therefore have not been used in the fit.

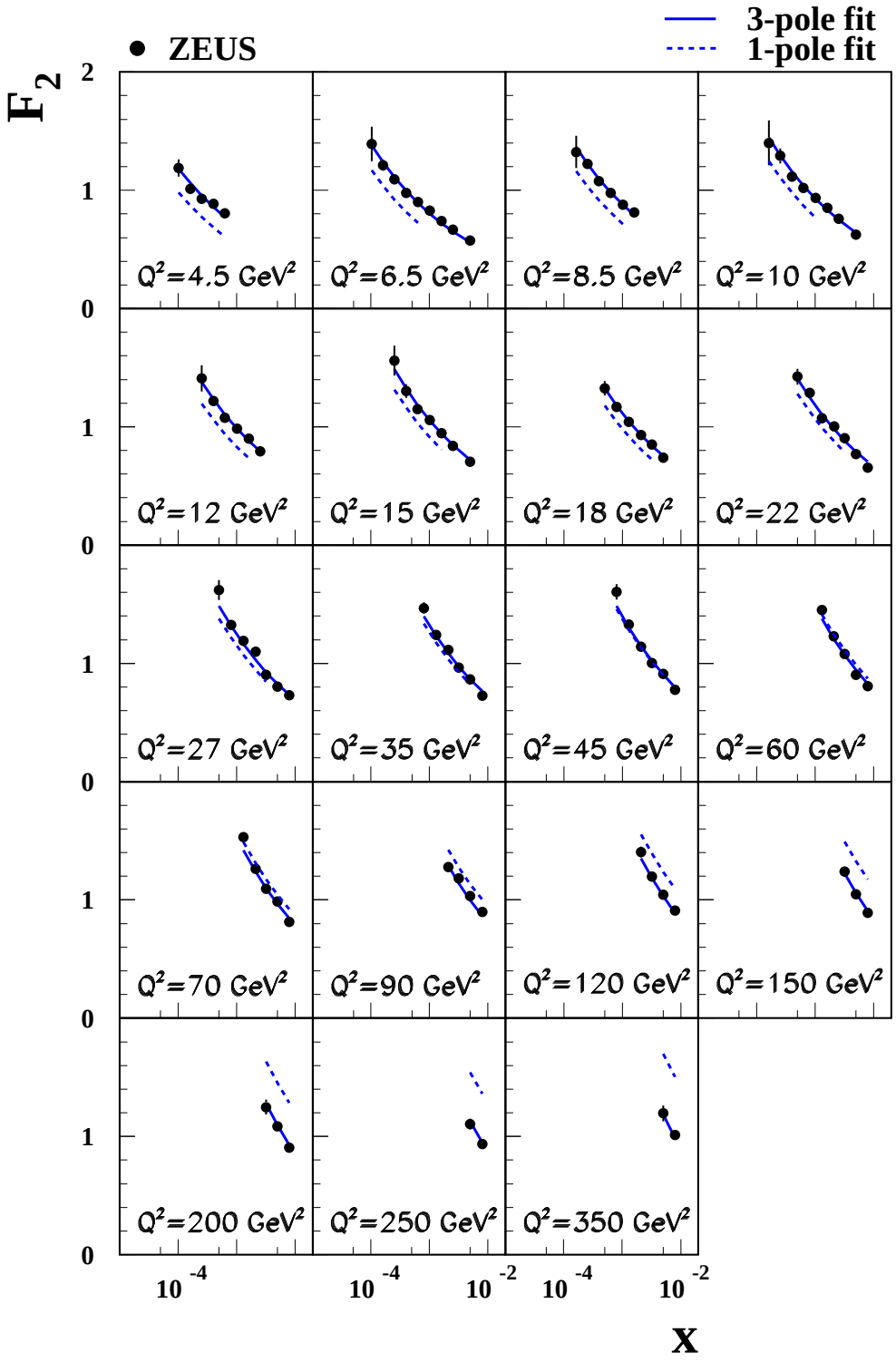


Figure 2: *Comparison of the HERA F_2 data with the 1- and 3-pole fits, shown as dashed and solid blue lines, respectively.*

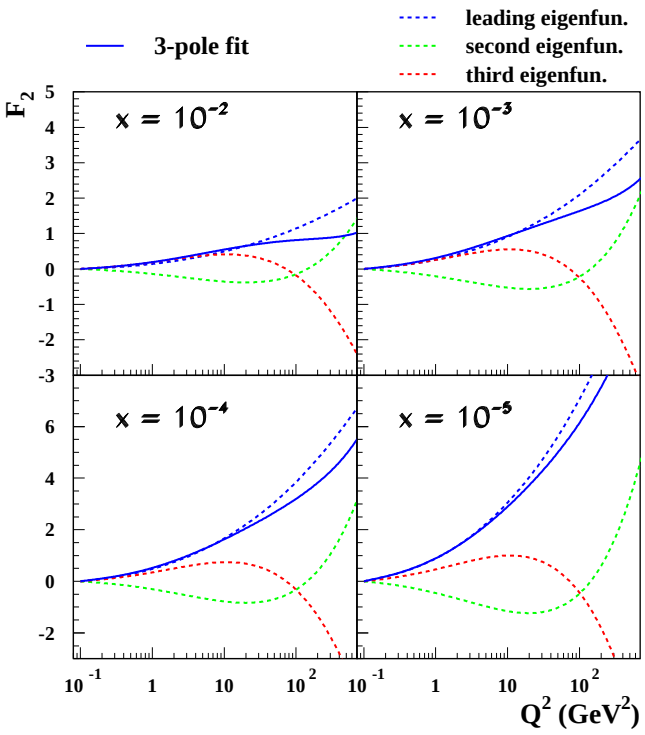


Figure 3: *The contributions to F_2 of the three eigenfunctions of the 3-pole fit.*

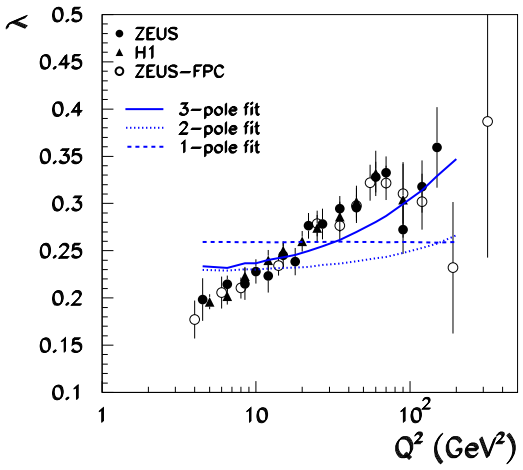


Figure 4: *The rate of rise λ, defined by $F_2 \propto (1/x)^\lambda$ at fixed Q^2, as determined in the three fits and in a direct phenomenological fit to the data.*

of Q^2, from $4 < Q^2 < 650$ GeV^2, using just three eigenfunctions and adjust 4 free constants: the phase η and the coefficients $a_{1,2,3}$ [5]. Important roles are played in the fit not only by the leading eigenfunction, but also by the pattern of cancellations between the sub-leading trajectories, which is very sensitive to the parameter η. For this reason, the quality of the fit is also very sensitive to the value of η. Thus, for $\eta = -0.3\pi$ the χ^2 grows to 142 for the 3 pole fit (instead 91.4 at the minimum), and at the extreme values of $\eta = -\pi/2$ and $\eta = 0$ the χ^2 values are 430 and 680, respectively. Consequently, the data determine the infrared phase quite precisely (within the theoretical framework described above) [6]: $\eta = -0.21 \pm 0.02\pi$ In turn, the leading eigenvalue is also precisely determined: $\omega = 0.26 \pm 0.01$. The relatively low value of this eigenvalue is responsible for the fact that, although the λ plot is reproduced by the 3-pole fit only in a qualitative way, we obtain a very good overall fit to the data.

To our knowledge, this is the first time that the discrete asymptotically-free BFKL Pomeron has been shown to fit the HERA data at low x and high Q^2. As such, we believe that it is also the first time that a parametrization of the Pomeron derived from first principles in QCD has been confronted successfully with experimental data. A natural next step would be to extend this comparison to include other low-x HERA data, including those on the diffractive production of vector mesons, etc. One could also envisage the development of a BFKL Pomeron calculus and its deployment to make predictions for both inclusive and exclusive phenomena at the LHC.

Acknowledgements

We express our warm appreciation for the inspiration and guidance offered to us by Lev Lipatov. In addition, HK thanks Jochen Bartels and Leszek Motyka for useful discussions.

References

[1] J.R. Forshaw and D.A. Ross, *Quantum Chromodynamics and the Pomeron* (Cambridge University Press, 1997).

[2] M. Derrick *et al.* [ZEUS Collaboration], *Phys. Lett.* B **315** (1993) 481.

[3] A. Donnachie and P.V. Landshoff *Nucl. Phys.* **B231** (1984) 189; **B244** (1984) 322; *Phys. Lett.* **B296** (1992) 227

[4] V.N. Gribov and L.N. Lipatov, *Sov. J. Nucl. Phys.* **15** (1972) 438;
L.N. Lipatov, *Sov. J. Nucl. Phys.* **20** (1975) 943;
G. Altarelli and G. Parisi, *Nucl. Phys,* **B126** (1977) 298;
Yu.L. Dokshitzer, *Sov. Phys. JETP* **46** (1977) 641.

[5] We recall that adding the fourth pole does not improve the fit.

[6] We emphasize that the value of η is linked to the arbitrary value chosen for the infrared scale, k_0, and furthermore that η is very sensitive to the theoretical input (e.g. the procedure employed for resumming the large NLO corrections).

[5] Y.Y Balitski and L.N. Lipatov, *Sov. J. Nucl. Phys.*, **28** (1978) 822;
V.S. Fadin, E.A. Kuraev and L.N. Lipatov, *Sov. Phys. JETP* **44** (1976) 443.

[6] See, e.g., B. Badelek, M. Krawczyk, K. Charchula and J. Kwiecinski, *Rev. Mod. Phys.* **64** (1992) 927;
J. Kwiecinski, A.D. Martin and A.M. Stasto, *Phys. Rev.* **D56** (1997) 3991.

[7] L.N. Lipatov, *Sov. Phys. JETP* **63** (1986) 904.

[8] V.S. Fadin and L.N. Lipatov, *Phys. Lett.* **B429** (1998) 127.

[9] G.P. Salam, *JHEP* **9807:019** (1998).

[10] L.N. Lipatov, private communication.

[11] J. Breitweg *et al.* [ZEUS Collaboration], Phys. Lett. B **487** (2000) 53;
C. Adloff *et al.* [H1 Collaboration], Eur. Phys. J. C **21** (2001) 33;
S. Chekanov *et al.* [ZEUS Collaboration], Eur. Phys. J. C **21** (2001) 443.

[12] H. Kowalski, L. Motyka and G. Watt, *Phys. Rev.* **D74** (2006) 074016.

[13] For an alternative point of view, see: E. Iancu, K. Itakura and S. Munier, *Phys. Lett.* B **590** (2004) 199.

[14] S. Chekanov *et al.* [ZEUS Collaboration], DESY 08-011, arXiv:0802.3017.